Distribution Ratios of Phosphorus Between CaO-FeO-SiO_2-Al_2O_3/Na_2O/TiO_2 Slags and Carbon-Saturated Iron

FENGSHAN LI, XIANPENG LI, SHUFENG YANG, and YANLING ZHANG

In order to effectively enhance the efficiency of dephosphorization, the distribution ratios of phosphorus between CaO-FeO-SiO_2-Al_2O_3/Na_2O/TiO_2 slags and carbon-saturated iron (L_P^{Fe-C}) were examined through laboratory experiments in this study, along with the effects of different influencing factors such as the temperature and concentrations of the various slag components. Thermodynamic simulations showed that, with the addition of Na_2O and Al_2O_3, the liquid areas of the CaO-FeO-SiO_2 slag are enlarged significantly, with Al_2O_3 and Na_2O acting as fluxes when added to the slag in the appropriate concentrations. The experimental data suggested that L_P^{Fe-C} increases with an increase in the binary basicity of the slag, with the basicity having a greater effect than the temperature and FeO content; L_P^{Fe-C} increases with an increase in the Na_2O content and decrease in the Al_2O_3 content. In contrast to the case for the dephosphorization of molten steel, for the hot-metal dephosphorization process investigated in this study, the FeO content of the slag had a smaller effect on L_P^{Fe-C} than did the other factors such as the temperature and slag basicity. Based on the experimental data, by using regression analysis, $\log L_P^{Fe-C}$ could be expressed as a function of the temperature and the slag component concentrations as follows:

$$\log L_P^{Fe-C} = 0.059(\text{pct CaO}) + 1.583\log(\text{TFe}) - 0.052(\text{pct SiO}_2) - 0.014(\text{pct Al}_2\text{O}_3) + 0.142(\text{pct Na}_2\text{O}) - 0.003(\text{pct TiO}_2) + 0.049(\text{pct P}_2\text{O}_5) + \frac{13{,}527}{T} - 9.87.$$

DOI: 10.1007/s11663-017-1023-8

I. INTRODUCTION

THE demand for high-quality steel with fewer impurities such as phosphorus is increasing. As is known, CaO-FeO-SiO_2-based slag tends to form during the dephosphorization process. While this slag generally has a high melting point, lower temperatures thermodynamically aid the removal of phosphorus from the metal melt. Therefore, fluxes are usually added to the slag to decrease its melting point, to improve the solubility of lime, and to enhance the kinetic efficiency of the dephosphorization process. CaF_2 was used widely in the past as an additive to reduce the melting point of the slag. However, these days, its use has been significantly restricted because of its toxic effects on human health. Increasing the FeO content is another common way of decreasing the melting point of the slag. However, this causes large iron losses. The effects of other additives such as Al_2O_3, Na_2O, MnO, and MgO on the properties of CaO-FeO-SiO_2 slag as well as its dephosphorization ability have been studied previously.[1–5] For instance, Diao[1] measured the melting temperature of CaF_2-free CaO-Fe_2O_3-Na_2O-Al_2O_3 dephosphorization slag using the hemisphere method. The results showed that both Na_2O and Al_2O_3 can decrease the melting temperature to less than 1473 K (1200 °C). Li *et al.*[2] reported the results of the dephosphorization of molten steel using MgO-saturated CaO-FeO_t-SiO_2 slag at 1823 K and 1873 K (1550 °C and 1600 °C). It was found that the addition of Na_2O to the MgO-saturated CaO-FeO_t-SiO_2 system increased the phosphorus distribution ratio in the slag. The addition of Al_2O_3 to the slag, in contrast, decreased the phosphorus distribution ratio. The phosphorus

FENGSHAN LI, XIANPENG LI, and YANLING ZHANG are with the State Key Laboratory of Advanced Metallurgy, University of Science and Technology Beijing, Beijing 100083, China. Contact e-mail: zhangyanling@metall.ustb.edu.cn SHUFENG YANG is with the School of Metallurgical and Ecological Engineering, University of Science and Technology Beijing, Beijing 100083, China.

Manuscript submitted October 24, 2016.
Article published online July 24, 2017.

distribution ratio for slags containing 0 to 5 mass pct Al_2O_3 and 0 to 1.75 mass pct Na_2O at 1873 K was 147 to 629 while that for slags containing 4.1 to 5.0 mass pct Al_2O_3 and 0 to 2.37 mass pct Na_2O at 1823 K was 202 to 247. For slags containing 21.28 to 23.59 mass pct Al_2O_3 and 0 to 4.25 mass pct Na_2O at 1823 K, the ratio was 41.5 to 84.8. Pak and Fruehan[3] reported that the addition of small amounts of Na_2O to conventional steelmaking slags greatly improved the dephosphorization rate. In the case of the $CaO-Al_2O_3-SiO_2$ slag used in ladle metallurgy for Al-killed steels, the addition of as little as 3 mass pct Na_2O increased the phosphorus distribution ratio at 1873 K (1600 °C) by a factor of 100. Jung *et al.*[4] reported that the phosphorus distribution ratio between $CaO-MgO_{sat}-SiO_2-Al_2O_3-Fe_tO-MnO-P_2O_5$ ladle slag and liquid iron increased with increases in the MnO contents at 1873 K (1600 °C). However, Simeonov and Sano[5] reported that MnO decreased the equilibrium phosphorus distribution between the $CaO-CaF_2-SiO_2-MnO$ system and carbon-saturated iron at 1573 K (1300 °C). Hence, the effect of adding MnO to slag on phosphorus removal is different for molten steel and carbon-saturated iron. Chen and He[6] reported that the distribution ratio of phosphorus between molten steel and $CaO-Al_2O_3-SiO_2-FeO-MgO-MnO-P_2O_5$ slags decreased markedly with increases in the MgO and MnO contents at 1873 K to 1943 K (1600 °C to 1670 °C). While these studies provided important basic data regarding the dephosphorization performances of various additives, they mainly focused on phosphorus removal from molten steel at temperatures as high as 1823 K to 1873 K (1550 °C to 1600 °C).

On the other hand, with respect to the currently employed convert steelmaking process, it is increasingly expected that a high phosphorus removal ratio will be achieved as early as possible, since the overoxidation caused by dephosphorization towards the end can have a significant negative effect on the cleanness of the molten steel; this is because a high oxygen content results in the presence of inclusions in large amounts. This further increases the refining burden and can cause the quality of the final product to deteriorate. Actually, phosphorus removal is thermodynamically favorable before massive decarburization occurs because of the relatively lower temperature and the high activity coefficient of phosphorus (which increases with an increase in the carbon content of the metal phase). The kinetics in this case worsen owing to the poor fluidity of the $CaO-FeO-SiO_2$-based dephosphorization slag at such low temperatures [1573 K to 1673 K (1300 °C to 1400 °C)], and fluxes such as Al_2O_3, Na_2O, MnO, and MgO are far more useful in this case. Simeonov and Sano[5] examined the phosphate capacities of $CaO-CaF_2-SiO_2-MnO-BaO$ and $CaO-CaF_2-SiO_2-MnO-Na_2O$ slags under hot-metal conditions. They found that BaO and Na_2O can raise the phosphate capacities of the slags. Liu *et al.*[7] reported that the addition of Al_2O_3 decreased phosphorus distribution ratio between $BaO-BaF_2-MnO-Al_2O_3$ slag and carbon-saturated ferromanganese at 1573 K (1300 °C). Li's experimental results showed that both Na_2O and K_2O can enhance the dephosphorization ability of $CaO-SiO_2-Fe_tO-P_2O_5$-based slags.[8] Danaei *et al.*[9] reported that the phosphorus distribution ratio of red-mud-based fluxes and carbon-saturated iron first increased and then decreased with an increase in the FeO content. Except for the studies described above, research efforts on the effects of Al_2O_3, Na_2O, and other similar materials on the ability of $CaO-FeO-SiO_2$-based slag to remove phosphorus from metal phases with high carbon contents have been lacking.

In order to effectively enhance the efficiency of dephosphorization of hot metals or that of the previous stage of the converter steelmaking process, the distribution ratios of phosphorus between $CaO-FeO-SiO_2-Al_2O_3/Na_2O/TiO_2$ slags and carbon-saturated hot metal were studied. First, the effects of Al_2O_3, Na_2O, and TiO_2 on the liquid areas of the $CaO-FeO-SiO_2$-based slag system were predicted thermodynamically. Then their effects on the distribution ratio of phosphorus between the slags and carbon-saturated molten iron were examined through equilibrium experiments performed in the laboratory.

II. LIQUID AREAS OF $CaO-SiO_2-FeO$ ($-Al_2O_3-Na_2O-TiO_2$) SLAG SYSTEM

The phase-diagram module of the software FactSage was used to simulate the liquid areas of the $CaO-SiO_2-FeO$ ($-Al_2O_3-Na_2O-TiO_2$) slag system at different temperatures. The liquid areas in the $CaO-SiO_2-FeO$ slag for temperatures of 1573 K to 1873 K (1300 °C to 1600 °C) are shown in Figure 1(a). As shown in the figure, the areas that are liquid at temperatures lower than 1673 K (1400 °C) require a binary basicity (pct CaO/pct SiO_2; in mass) of 0.6 to 1.0. Further, the melting point of the $CaO-SiO_2-FeO$ system decreases with an increase in the FeO content. This supports the conclusion that the fluidity of the slag as well as the dissolution of lime in it is improved with an increase in its FeO content. In addition, it suggests that a melting point lower than 1673 K (1400 °C) but corresponding to a binary basicity higher than 2.0 (the basicity for ensuring a higher dephosphorization efficiency) is impossible to achieve in the case of the $CaO-SiO_2-FeO$ slag system unless effective fluxes such as CaF_2 are used. The effects of Al_2O_3, Na_2O, and TiO_2 (5 pct) on the 1573 K (1300 °C) liquid areas of the $CaO-FeO-SiO_2$ slag are shown in Figure 1(b). As shown in the figure, with the addition of Na_2O and Al_2O_3, the liquid areas increase in size significantly, with Na_2O having a more pronounced effect than Al_2O_3; TiO_2, on the other hand, has little effect. Figures 1(c) and (d) show the dependence of the 1573 K (1300 °C) liquid area on the Al_2O_3 and Na_2O contents, respectively. It can be seen that the 1573 K (1300 °C) liquid area of the $CaO-SiO_2-FeO$ slag increases sharply in size with an increase in the Na_2O content from 2 to 8 pct as well as with an increase in the Al_2O_3 content from 5 to 15 pct. In addition, the liquid area moves towards the direction corresponding to an increase in the CaO content but a decrease in the FeO content. This implies that the addition of Al_2O_3 or Na_2O

can increase the solubility of lime and reduce iron loss during steelmaking, as a lower melting point can be achieved even at a lower FeO content. However, it also needs to be noted that too high an Al_2O_3 content would have a negative effect. As shown in Figure 1(c), when the Al_2O_3 content is as high as 20 pct, the liquid region is divided into two parts and becomes much smaller. These calculations showed that, when used in the right concentrations, Al_2O_3 or Na_2O can behave as fluxes in the CaO-SiO_2-FeO slag, especially under conditions where the binary basicity is high.

III. EXPERIMENTAL

A. *Principles*

Direct measurements of the phosphorus distribution ratio between CaO-FeO-SiO_2-based slag and a carbon-saturated liquid metal cannot be performed since the FeO in the slag could react with the carbon dissolved in the liquid metal. Accordingly, the technique developed by Sano and colleagues[10] and Ito and Sano[11] was employed in this study for measuring the phosphorus distribution ratios between the various slags and iron foil instead of those between the slags and hot metal. The former values were then converted into the latter. In this manner, the phosphorus distribution ratios between the CaO-FeO-SiO_2-based slags and carbon-saturated hot metal could be obtained.

When solid γ-iron is in equilibrium with a slag, the hot metal, which has the same chemical potential for phosphorus as that of γ-iron, should be also in equilibrium with the slag with respect to phosphorus. The phosphorus distribution ratios between the slag and the solid iron can be converted into those between the slag and the carbon-saturated hot metal by multiplying the

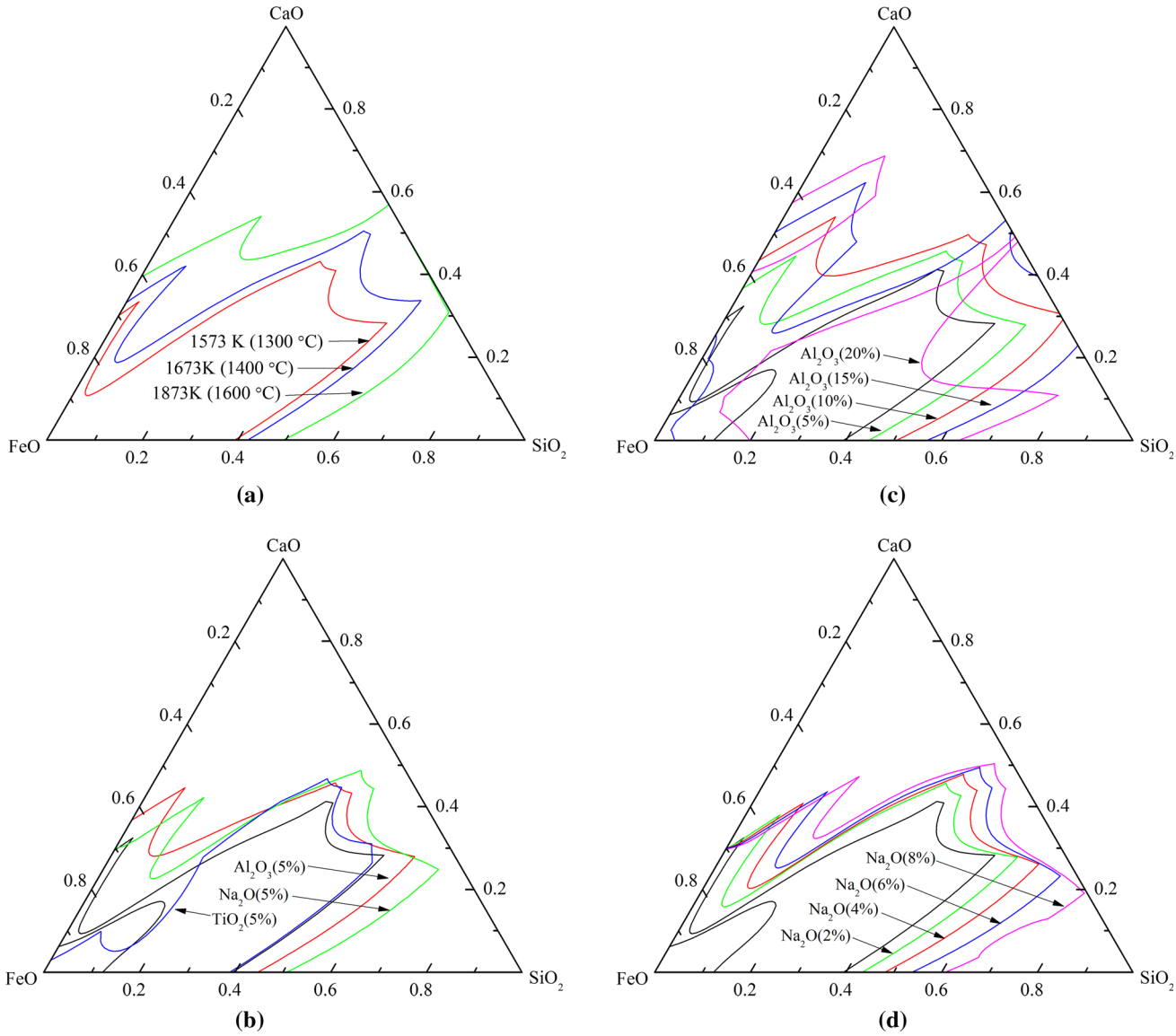

Fig. 1—Liquid regions of CaO-FeO-SiO_2-based slags: (*a*) liquid areas for different temperatures, (*b*) effect of slag compositions at 1573 K (1300 °C), (*c*) effect of Al_2O_3 content at 1573 K (1300 °C), and (*d*) effect of Na_2O content at 1573 K (1300 °C).

distribution ratio of phosphorus between the solid iron and the hot metal as long as their oxygen partial pressures are similar.

After keeping the slag samples with the target compositions and a piece of foil of solid iron in the equilibrium state in an ARMCO iron crucible in a pure argon atmosphere for an appropriate period, the phosphorus distribution ratio between the slag and the solid iron foil, $L_P^{Fe-\gamma}$, could be obtained as follows:

$$L_P^{Fe-\gamma} = \frac{(\text{pct P})}{[\text{pct P}]^{Fe-\gamma}}, \quad [1]$$

where (pct P) and [pct P]$^{Fe-\gamma}$ are the phosphorus contents in the slag and the iron foil, respectively.

The chemical potential of phosphorus in solid iron and carbon-saturated iron can be written as follows[12–14]:

$$\mu_P^{Fe-\gamma} = \mu_{P(l)}^{\theta} + RT \ln \gamma_P^{Fe-\gamma} \cdot X_P^{Fe-\gamma}, \quad [2]$$

$$\mu_P^{Fe-C} = \mu_{P(1\ pct)}^{\theta} + RT \ln \gamma_P^{Fe-C} \cdot X_P^{Fe-C}, \quad [3]$$

where $X_P^{Fe-\gamma}$, $\mu_P^{Fe-\gamma}$, and $\gamma_P^{Fe-\gamma}$ represent the molar fraction of phosphorus, chemical potential of phosphorus, and activity coefficient of phosphorus in pure solid iron, respectively, X_P^{Fe-C}, μ_P^{Fe-C}, and γ_P^{Fe-C} represent the molar fraction of phosphorus, chemical potential of phosphorus, and activity coefficient of phosphorus in carbon-saturated iron, respectively, $\mu_{P(l)}^{\theta}$ represents the chemical potential of phosphorus in a standard superheated liquid state, $\mu_{P(1\ pct)}^{\theta}$ represents the chemical potential of phosphorus in a standard state of 1 pct solution of phosphorus in liquid iron.

Under same experimental conditions, the values of $\mu_P^{Fe-\gamma}$ and μ_P^{Fe-C} are equal. Therefore, the equation for the phosphorus contents can be written as follows[12,13]:

$$\ln \frac{[\text{pct P}]^{Fe-\gamma}}{[\text{pct P}]^{Fe-C}} = -16.594 - 2.4029 \times 10^{-5} T + \frac{9538}{T} + \frac{12{,}505}{T^2} + 0.98356 \ln T + \ln \gamma_P^{Fe-\gamma}, \quad [4]$$

where [pct P]$^{Fe-C}$ and T are the phosphorus content in the iron foil and the temperature (K), respectively. Accordingly, the ratio of L_P^{Fe-C} to $L_P^{Fe-\gamma}$, expressed as H in Eq. [5], varies with the temperature; H is 0.413, 0.397, and 0.383 at 1573 K, 1623 K, and 1673 K (1300 °C, 1350 °C, and 1400 °C), respectively.

$$H = \frac{L_P^{Fe-C}}{L_P^{Fe-\gamma}}, \quad [5]$$

where L_P^{Fe-C} is the phosphorus distribution ratio between the slag and carbon-saturated liquid iron.

Therefore, by using the measured phosphorus contents in the slag and the iron foil, the phosphorus distribution ratio between the slag and carbon-saturated iron, L_P^{Fe-C}, can be obtained.

B. *Samples*

The material and chemical reagents used included iron foil, CaO, Fe_3O_4, SiO_2, Al_2O_3, Na_2SiO_3, TiO_2, and P_2O_5. The iron foil was of high-purity iron (thickness of 0.1 mm, mass Fe >99.999 pct), and the P content of the iron foil was lower than 0.0001 mass pct. FeO was produced by reducing Fe_3O_4 in a CO gas atmosphere (flow rate 3 L/min) for 5 hours at 1173 K (900 °C) and subsequently quenching the sample in an atmosphere of pure argon. After being cooled, the solid material was ground to a particle size of 200 μm. The sample was analyzed by X-ray diffraction (XRD) analysis; the XRD spectrum is shown in Figure 2. The pattern confirmed that high-purity FeO was obtained. Na_2O was added in the form of Na_2SiO_3 to prevent it from evaporating during the high-temperature process.[3] The P_2O_5 content was kept the same for all the experiments in a group but was changed between groups of experiments. CaO was dried in a drying box at 393 K (120 °C) for 24 hours before use.

The based slags were formed by mixing CaO, FeO, SiO_2, P_2O_5, Al_2O_3, Na_2SiO_3, and TiO_2 in a porcelain mortar. After being mixed well, the slags were dried at 393 K (120 °C) for 24 hours and then kept in a sealed container. The based slags were then formed into cylindrical pellets with a diameter of 20 mm using a presser, which applied a pressure of 20 MPa for 120 seconds.

Table I lists the compositions of the various slags used and those of the metal phase. During experiments 1 to 15, the quaternary CaO-FeO-SiO_2-Al_2O_3/Na_2O/TiO_2 slag systems were used to elucidate the effects of Al_2O_3, Na_2O, and TiO_2 on the phosphorus distribution ratio between the slags and carbon-saturated iron. For experiments 16 to 54, the six-component slag system CaO-FeO-SiO_2-Al_2O_3-Na_2O-TiO_2 was used, and the effects of the temperature, binary basicity, and FeO content were examined.

C. *Apparatus Used and Procedure*

A schematic diagram of the experimental apparatus used is given in Figure 3. The experiment setup includes a horizontal electric resistance furnace, a water-cooling system, and an associated purification plant for argon gas. The furnace was equipped with $MoSi_2$ heating elements and was controlled by a proportional–integral–derivative controller with a Pt-30 pct Rh/Pt-6 pct Rh thermocouple as the sensor; the thermocouple was calibrated before use. The temperature control range of the furnace was 298 K to 1973 K (25 °C to 1700 °C) and was controlled within ±1 K (1 °C). The end of reaction tube was kept at 298 K (25 °C) using the water-cooling system, which was filled with circulating water. The equilibrium experiments were carried out in an Ar atmosphere, and it was necessary to purify the Ar gas before it was introduced into the reaction tube. The associated purification train for argon consisted of allochroic silica gel for dehydration and magnesium and copper chips [heated to 773 K (500 °C)] for deoxidation.

Cylindrical pellets containing 20 g of the slag were placed in the ARMCO iron crucible (mass Fe >99.8 pct, outer diameter of 27 mm, inner diameter of 25 mm, height of 31 mm). After the slag pellets had been placed in the crucible, a 2 g piece of iron foil was cut into smaller pieces, which were placed in the gap between every two pellets. Each porcelain boat could hold five iron crucibles and was placed in the heating zone after being tied with a molybdenum wire. Next, the Ar gas flow was turned on (flow rate 400 mL/minute) and the furnace was switched on. The target temperatures were 1573 K, 1623 K, and 1673 K (1300 °C, 1350 °C, and 1400 °C). The melt was equilibrated for 8 to 12 hours. Ito and Sano[11] have reported that a period of this length is enough for equilibrium to be established. Therefore, we used an equilibrium period of 12 hours. After equilibrium had been reached, the porcelain boat was quickly pulled into the cooling zone in an atmosphere of argon gas. The samples were then allowed to cool and subsequently removed from the furnace.

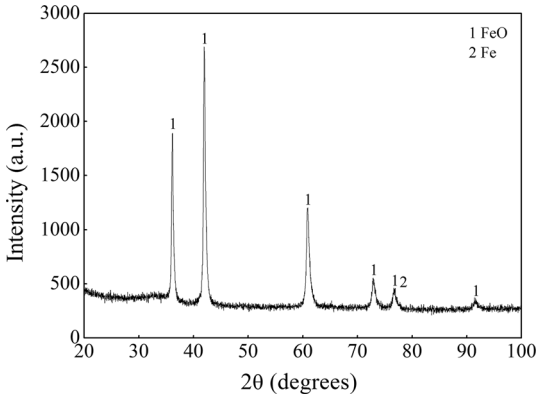

Fig. 2—XRD spectrum of prepared FeO sample.

D. *Analysis*

After being cooled, the iron foil pieces were separated from the slag. The slag was ground to a particle size of 200 μm and analyzed using X-ray fluorescence measurements. Since the presence of even a small amount of the slag in the iron phase can cause significant errors in the phosphorus content, the iron foil pieces were carefully polished with a stainless steel brush. They were then cleaned ultrasonically in a citric acid/acetone mixture and subsequently in deionized water. The P content of the cleaned iron foil pieces was analyzed by molybdenum blue colorimetry, and the $L_P^{Fe-\gamma}$ value was determined. Then L_P^{Fe-C} could be determined using Eq. [5], as shown above.

IV. RESULTS AND DISCUSSION

A. *Effect of Temperature on* L_P^{Fe-C}

The temperature dependence of $\log L_P^{Fe-C}$ is shown in Figure 4. The data in Figure 4(a) are the results of experiments 36 to 40 and 50 to 54 in Table I; for these experiments, the slag compositions were nearly similar. Figure 4(b) shows the dependence of L_P^{Fe-C} on the temperature in the case of the entire six-component slag system (CaO-FeO-SiO_2-Al_2O_3-Na_2O-TiO_2), whose compositions varied significantly (experiments 16 to 54 in Table I). It can be seen from Figure 4(a) that, for similar slag compositions, L_P^{Fe-C} decreases with an increase in the temperature. This agreed well with the thermodynamic

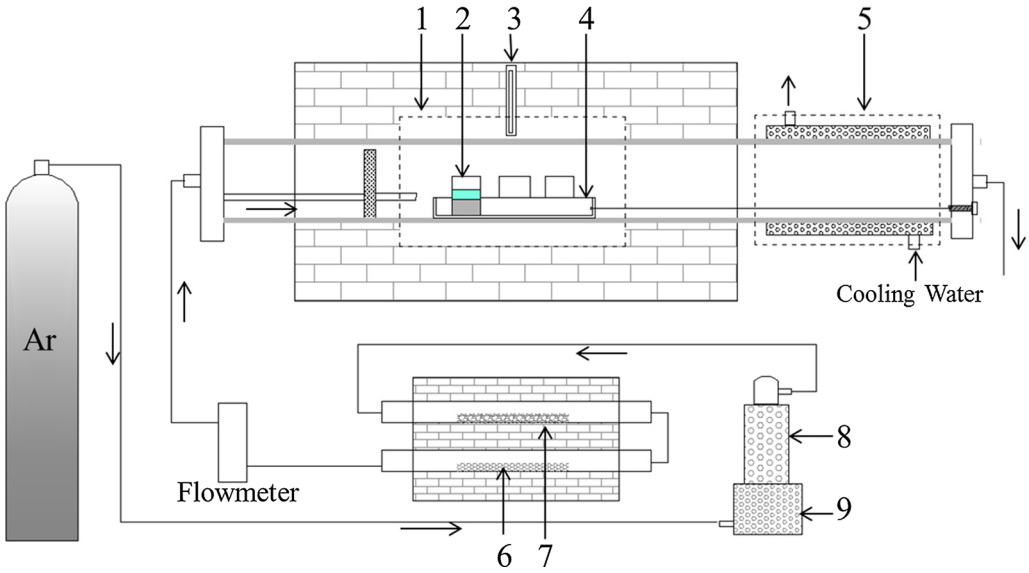

(1-heating zone; 2-iron crucible; 3-thermocouple; 4-porcelain boat made of Al_2O_3; 5-water-cooling device; 6-magnesium pieces; 7-copper pieces; 8-molecular sieve; 9-allochroic silica gel)

Fig. 3—Schematic diagram of experiment setup.

Table I. Slag and Metal-Phase Compositions After Equilibration and L_P Values

		Flux and Metal-Phase Composition After Equilibration (Wt. Pct)											
Nos.	Variables	CaO	FeO	SiO_2	Al_2O_3	Na_2O	TiO_2	(P)	$[P]^{Fe-\gamma}$	R	$L_P^{Fe-\gamma}$	L_P^{Fe-C}	$\log L_P^{Fe-C}$
1	Al_2O_3	29.846	34.050	29.103	0	0	0	2.105	0.0050	1.00	421.0	173.9	2.240
2		29.286	33.511	28.712	3.348	0	0	2.103	0.0078	1.0	269.6	111.3	2.047
3		28.145	32.426	28.112	6.146	0	0	2.137	0.0130	1.00	164.4	67.9	1.832
4		26.754	31.135	26.963	10.052	0	0	2.091	0.0190	1.0	110.1	45.5	1.658
5		25.430	30.106	25.643	13.418	0	0	2.202	0.0230	1.00	88.1	36.4	1.561
6	Na_2O	28.851	31.945	28.281	0	0.082	0	4.507	0.0270	1.0	166.9	68.9	1.839
7		27.853	31.453	28.206	0	1.608	0	4.575	0.0200	1.00	228.7	94.5	1.975
8		27.311	30.705	27.670	0	3.348	0	4.623	0.0100	1.0	462.3	190.9	2.281
9		26.288	29.001	26.625	0	4.949	0	4.701	0.0085	1.00	553.1	228.4	2.359
10		25.913	28.961	26.555	0	6.944	0	4.903	0.0067	1.0	731.9	302.3	2.480
11	TiO_2	29.846	34.050	29.103	0	0	0	2.105	0.0050	1.00	421.0	173.9	2.240
12		29.508	33.254	29.401	0	0	2.060	2.219	0.0057	1.0	389.3	160.8	2.206
13		29.488	33.603	28.537	0	0	4.025	2.174	0.0062	1.00	350.7	144.8	2.161
14		27.675	32.075	28.837	0	0	5.895	2.149	0.0065	1.0	330.6	136.5	2.135
15		27.058	30.796	28.221	0	0	7.810	2.235	0.0073	1.00	306.1	126.4	2.102
16	FeO	29.411	12.309	28.220	11.768	4.329	2.273	4.590	0.0440	1.0	104.3	43.1	1.634
17		25.243	20.403	26.499	11.114	3.925	1.969	4.615	0.0420	1.00	109.9	45.4	1.657
18		21.174	29.552	23.495	9.721	3.635	1.590	4.603	0.0350	0.9	131.5	54.3	1.735
19		18.153	37.516	19.671	7.339	3.487	1.317	4.463	0.0190	0.90	234.9	97.0	1.987
20		14.311	45.269	17.201	6.380	3.000	1.037	4.554	0.0250	0.8	182.2	75.2	1.876
21	Basicity, R	19.662	35.965	20.898	7.873	3.055	1.402	4.417	0.0130	0.9	339.7	140.3	2.147
22		17.399	36.746	22.695	7.671	3.126	1.377	4.413	0.0320	0.8	137.9	57.0	1.756
23		14.781	37.919	24.884	7.357	3.009	1.404	4.422	0.0700	0.6	63.2	26.1	1.416
24		11.413	38.558	28.263	7.151	2.748	1.399	4.438	0.1800	0.4	24.7	10.2	1.008
25		7.101	40.318	32.184	7.061	2.658	1.365	4.407	0.6200	0.2	7.1	2.9	0.468
26	T = 1573 K	15.703	27.553	16.864	14.216	5.025	6.065	4.514	0.027	0.9	167.2	69.0	1.839
27		19.11	26.844	20.103	14.109	3.361	4.219	5.226	0.033	1.0	158.4	65.4	1.816
28		24.713	22.533	27.328	10.270	2.329	2.199	4.517	0.064	0.9	70.6	29.1	1.465
29		21.073	21.060	22.493	17.666	3.291	3.199	4.762	0.075	0.9	63.5	26.2	1.419
30		18.081	29.394	19.256	13.729	3.516	4.186	5.047	0.030	0.9	168.2	69.5	1.842
31		14.261	33.838	15.813	11.445	5.795	5.965	5.067	0.014	0.9	361.9	149.5	2.175
32		22.834	26.933	23.828	3.410	5.090	6.214	4.972	0.011	1.0	452.0	186.7	2.271
33		21.510	24.975	21.949	10.317	4.172	5.178	5.086	0.028	1.0	181.6	75.0	1.875
34		20.048	23.390	20.978	16.314	2.523	5.315	4.857	0.063	1.0	77.1	31.8	1.503
35		19.695	29.368	20.536	13.669	1.688	2.204	5.058	0.055	1.0	92.0	38	1.580
36	T = 1623 K	18.128	29.837	19.793	14.018	4.760	2.098	4.702	0.032	0.9	147	58.3	1.766
37		17.846	25.156	19.122	14.030	8.788	2.022	4.463	0.012	0.9	371.9	147.7	2.169
38		25.863	24.573	23.954	8.311	4.014	2.178	4.723	0.038	1.1	124.3	49.3	1.693
39		27.827	25.287	23.367	6.245	3.075	3.225	4.678	0.025	1.2	187.1	74.3	1.871
40		29.440	26.278	23.270	6.279	1.616	2.161	4.678	0.030	1.3	155.9	61.9	1.792
41		27.730	22.143	22.627	9.883	7.822	5.934	1.666	0.0035	1.2	499.0	198.1	2.297
42		30.769	22.127	19.256	9.992	7.993	5.962	1.677	0.0021	1.6	831.7	330.2	2.519
43		33.440	22.275	16.546	9.875	7.984	5.994	1.682	0.0015	2.0	1164.3	462.2	2.665
44		35.294	22.322	14.706	9.934	7.892	5.973	1.671	0.0012	2.4	1455.4	577.8	2.762
45		36.312	15.132	18.143	10.946	8.757	6.568	1.702	0.0022	2.0	793.9	315.2	2.499
46		34.216	20.334	17.027	10.270	8.016	6.106	1.713	0.002	2.0	873.2	346.7	2.540
47		28.630	31.011	14.756	8.919	7.335	5.351	1.685	0.0016	1.9	1091.6	433.3	2.637
48		25.023	40.586	12.211	7.568	6.154	4.541	1.696	0.0014	2.0	1247.5	495.3	2.695
49		20.321	50.643	10.160	6.216	4.973	3.730	1.716	0.002	2.0	873.2	346.7	2.540
50	T = 1673 K	18.521	28.224	20.540	14.107	4.900	2.088	4.914	0.065	0.9	75.6	29.0	1.462
51		16.101	27.246	20.416	14.912	8.328	2.201	4.394	0.034	0.8	129.2	49.5	1.695
52		25.960	25.579	23.395	7.314	3.874	2.169	4.937	0.07	1.1	70.5	27.0	1.432
53		27.866	24.257	23.951	6.523	2.992	3.213	4.678	0.058	1.2	80.7	30.9	1.490
54		29.532	25.680	23.830	6.432	1.559	2.161	4.544	0.061	1.2	74.5	28.5	1.455

Annotation: R = (pct CaO)/(pct SiO_2).

predictions for the dephosphorization reaction, which is exothermic and thus aided by lower temperatures.

However, this trend did not hold for the data shown in Figure 4(b). At temperatures lower than 1623 K (1350 °C), a few samples (encircled by a solid line) resulted in higher phosphorus distribution ratios than those at a temperature of 1573 K (1300 °C). The reason for this could be the fact that these samples had binary basicities as high as 1.2 to 2.4 (experiments 41 to 49 in Table I). At a lower temperature, namely, 1573 K (1300 °C), the samples encircled by a dashed line in Figure 4(b) resulted in much lower phosphorus distribution ratios than those at high temperatures such as 1623 K and 1673 K (1350 °C and 1400 °C). These samples exhibited binary basicities as low as 0.2 to 0.9 (experiments 21 to 25 in Table I). The binary basicities of all the samples except those used in experiments 41 to 49 and 21 to 25 were 0.8 to 1.3. This suggested that, with respect to the dephosphorization of hot metal, the basicity of the slag used is more important than the temperature: high slag basicity tends to result in a high phosphorus distribution ratio even at higher temperatures (samples encircled by a solid line in Figure 4(b)), which do not benefit dephosphorization thermodynamically, while a lower slag basicity results in a lower phosphorus distribution ratio even at lower temperatures (samples encircled by a dashed line in Figure 4(b)).

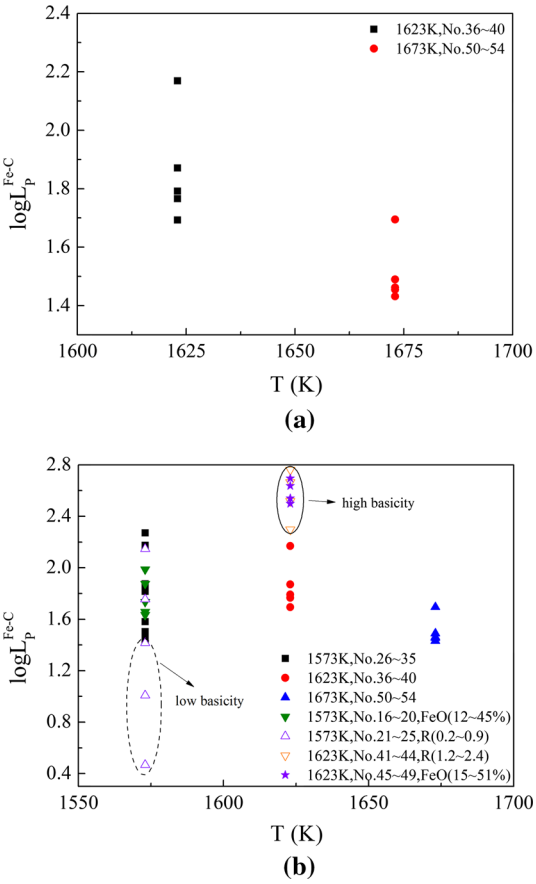

Fig. 4—Effect of temperature on $\log L_P^{Fe-C}$: (*a*) samples for experiments 36 to 40 and 50 to 54 in Table I and (*b*) samples for experiments 16 to 54 in Table I.

B. *Effect of Binary Basicity of Slag*

The effect of the (pct CaO)/(pct SiO_2) ratio on $\log L_P^{Fe-C}$ is shown in Figure 5. The data in Figure 5(a) are the results for two groups of experiments (21 to 25 and 41 to 44 in Table I) for which the compositions were similar (FeO-Al_2O_3-Na_2O-TiO_2) but the (pct CaO)/(pct SiO_2) values were different. This suggested that $\log L_P^{Fe-C}$ increases sharply with an increase in the binary basicity. This would be consistent with the results of a study by Im *et al.*,[12] who investigated the phosphorus distribution ratio between carbon-saturated iron and slags with basicities of 0.5 to 1.0 at temperatures lower than 1573 K (1300 °C). Further, this suggested that the increase in the L_P^{Fe-C} value with an increase in the binary basicity is much larger at low temperatures and low basicities [black solid squares, 1573 K (1300 °C), R = 0.2 to 0.9, experiments 21 to 25 in Table I] than that at high temperatures and high basicities [red solid circles, 1623 K (1350 °C), R = 1.2 to 2.4, experiments 41 to 44 in Table I]. Similar tendencies have been observed in previous studies as well.[12,15] For instance, the increase in the value of the phosphorus distribution ratio observed by Ishii and Fruehan[15] with increasing basicity was much lower than that reported by Im *et al.*[12] (see Figure 5(a)).The former study was performed using slags with basicities of 2.0 to 6.7 and molten steel with an extremely low carbon content at 1843 K and 1873 K (1570 °C and 1600 °C), while the latter involved phosphorus distribution between slags and carbon-saturated iron with basicities of 0.5 to 1.0 at a lower temperature, namely, 1573 K (1300 °C).

The data in Figure 5(b) show the dependence of the phosphorus distribution ratio of all the six-component slag system samples used in this study (experiments 16 to 54, Table I) on the total binary basicity under different temperatures. Irrespective of the FeO, Al_2O_3, and Na_2O contents and the temperature, $\log L_P^{Fe-C}$ showed a strong dependence on the (pct CaO)/(pct SiO_2) value of the slag used. This indicated that the slag basicity is a primary factor affecting the phosphorus distribution ratio between the slag and the hot-metal phase. In addition, the data in Figure 5(b) also suggested that, for the samples for which (pct CaO)/(pct SiO_2) was approximately 1.0, the $\log L_P^{Fe-C}$ value was relatively smaller [see yellow asterisks; for these samples, the measurements were performed at 1673 K (1400 °C), which was the highest temperature used during the experiments]. This indicated that the temperature also has a strong effect on the dephosphorization process, with a high temperature limiting the dephosphorization performance.

C. *Effect of Na_2O Content in Slag*

The data in Figure 6(a) show the dependence of $\log L_P^{Fe-C}$ on the Na_2O content of the slag used; the contents of the other slag constituents were changed only marginally while the temperature was kept constant (experiments 6 to 10 in Table I, quaternary slags). As shown in the figure, the phosphorus distribution ratio

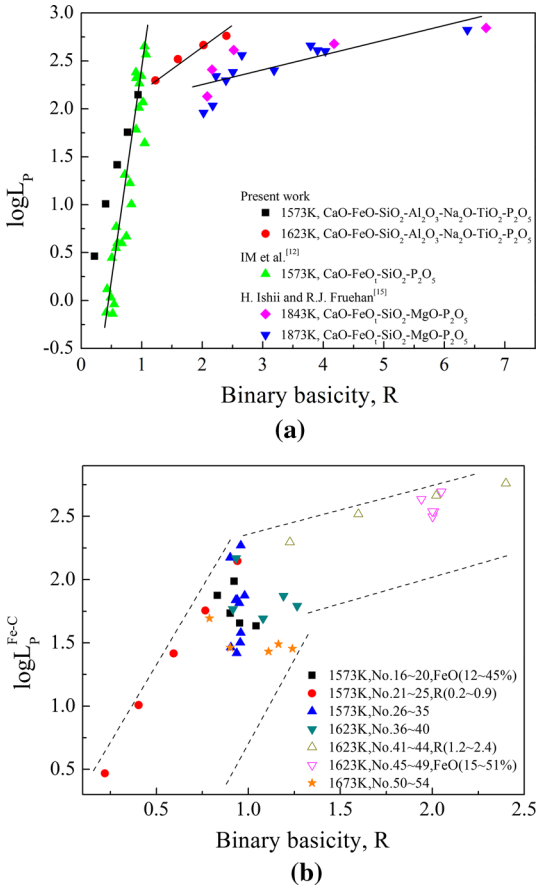

Fig. 5—Dependence of $\log L_P^{Fe-C}$ on slag binary basicity: (*a*) samples for experiments 21 to 25 and 41 to 44 in Table I and (*b*) samples for experiments 16 to 54 in Table I.

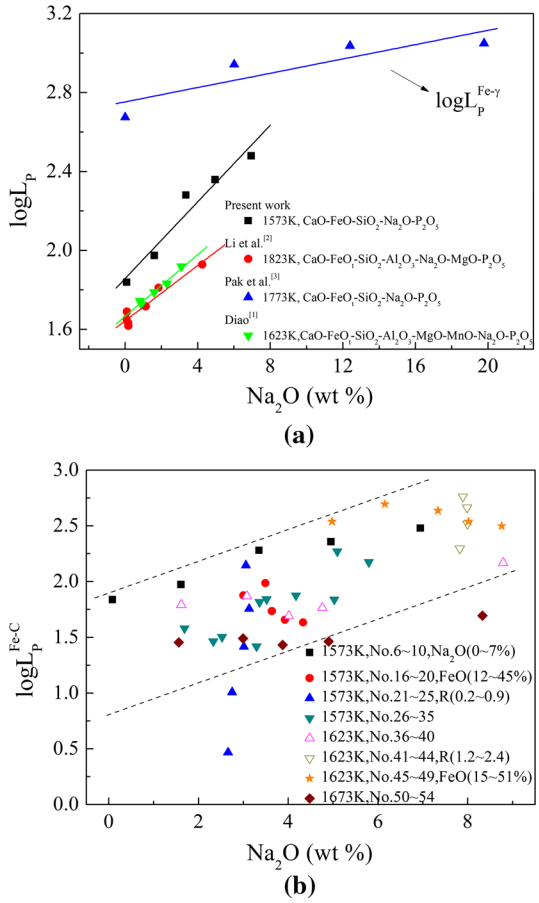

Fig. 6—Effect of Na_2O on $\log L_P$: (*a*) samples for experiments 6 to 10 in Table I and (*b*) samples for experiments 6 to 10 and 16 to 54 in Table I.

between the slag and the metal phase increases linearly with increases in the Na_2O content. When the Na_2O content is increased by 6.94 pct, the L_P^{Fe-C} value increases by approximately 4.4 times. The same trend has been observed in previous studies as well.[1–3] Pak and Fruehan[3] observed a much higher L_P value even at a temperature as high as 1773 K (1500 °C). This was because what they measured was $L_P^{Fe-\gamma}$ rather than L_P^{Fe-C}; the former is usually twice as large as the latter, as can be seen from Eq. [5].

The dependence of $\log L_P^{Fe-C}$ on the Na_2O content for all the six-component slag system samples (experiments 16 to 54 in Table I) for the various temperatures and slag compositions investigated in this study is shown in Figure 6(b). As shown in the figure, there is a significant variation in the L_P^{Fe-C} value even for the same Na_2O content; this was caused by the variations in the other factors such as the basicity and temperature. However, an obvious trend can still be observed, which is that $\log L_P^{Fe-C}$ increases with an increase in the Na_2O content. This suggests that the Na_2O content also has a significant effect on the hot-metal dephosphorization. Na_2O has a higher alkalinity than that of CaO. Thus, it also has a greater dephosphorization ability.[16] Further, Na_2O can also reduce the melting point of slags.[13] Finally, it has been reported that the addition of Na_2CO_3 to refining slags results in simultaneous dephosphorization and desulfurization.[17–19]

D. *Effects of Al_2O_3/TiO_2 Contents*

The effect of the Al_2O_3 content on $\log L_P^{Fe-C}$ under conditions where the concentrations of the rest of the slag constituents as well as the temperature are kept constant (experiments 1 to 5 in Table I, quaternary slags) is shown in Figure 7(a). As shown in the figure, $\log L_P^{Fe-C}$ decreases linearly with an increase in the Al_2O_3 content of the slags. This is in keeping with the results reported by Diao.[1] Further, Wrampelmeyer *et al.*[20] reported that the phosphorus distribution ratio between CaO-saturated slag and pure molten iron decreases slightly with an increase in the Al_2O_3 content; however, the ratio decreases sharply when the Al_2O_3 content is higher than 25 pct, as shown as Figure 7(a).

The dependence of $\log L_P^{Fe-C}$ on the Al_2O_3 content for all the six-component slag system samples (experiments 16 to 54 in Table I) for the different temperatures investigated in this study is shown in Figure 7(b). As shown in the figure, the value of $\log L_P^{Fe-C}$ varies significantly even when the Al_2O_3 content is kept

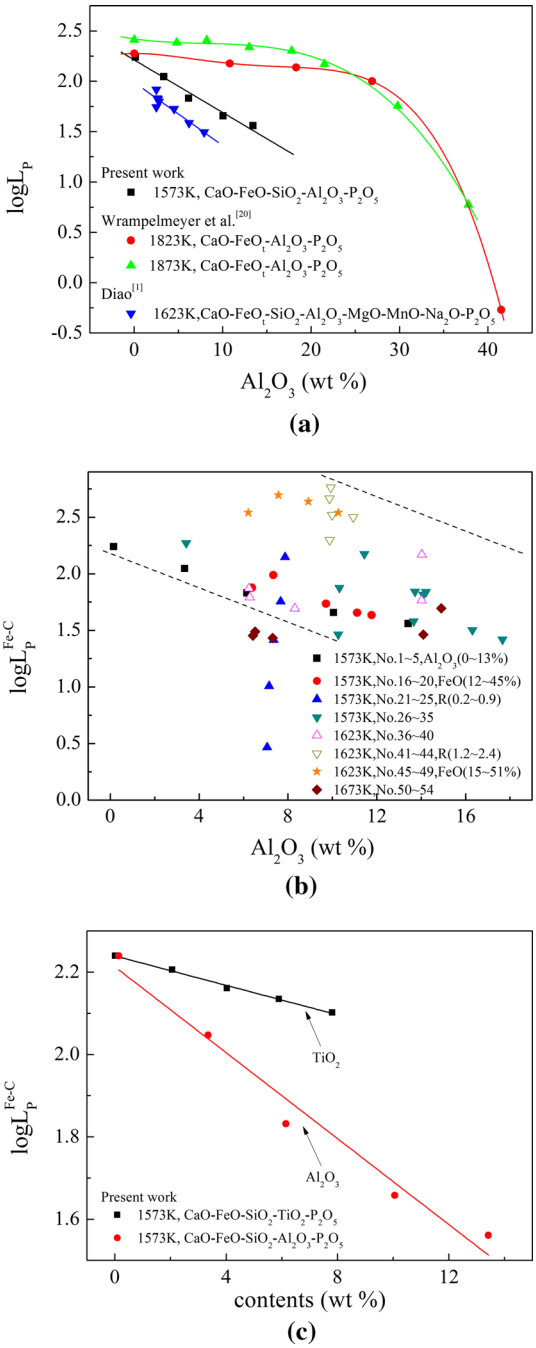

Fig. 7—Effects of Al_2O_3 and TiO_2 on $\log L_P$: (*a*) samples for experiments 1 to 5 in Table I, (*b*) samples for experiments 1 to 5 and 16 to 54 in Table I, and (*c*) samples for experiments 1 to 5 and 11 to 15 in Table I.

constant. However, it can also be seen that, overall, $\log L_P^{Fe-C}$ decreases with an increase in the Al_2O_3 content. This indicated that the Al_2O_3 content of the slag used also affects the dephosphorization of hot metal. According to the ionic theory of slags, PO_4^{3-} ions replace SiO_4^{4-} ions and then precipitate in the form of $Ca_3(PO_4)_2$ during the dephosphorization process. At the same time, SiO_4^{4-} ions are also replaced by AlO_4^{5-} ions. If the Al_2O_3 content is very high, the precipitation of PO_4^{3-} will be suppressed. This will have a negative effect on phosphorus removal. In this case, Al_2O_3 exhibits the characteristics of an acidic oxide.[1]

The data in Figure 7(c) show the dependence of L_P^{Fe-C} on the TiO_2 and Al_2O_3 contents for the quaternary slag samples used in this study (experiments 1 to 5 and 11 to 15 in Table I) for the same temperature. It can be seen that $\log L_P^{Fe-C}$ decreases slightly with an increase in the TiO_2 content of the slags. However, compared to the effect of the Al_2O_3 content, that of the TiO_2 content on dephosphorization is significantly less pronounced.

E. *Effect of FeO Content*

The effect of the FeO content in the slags on L_P^{Fe-C} is shown in Figure 8(a) (data from experiments 16 to 20 and 45 to 49 in Table I); the concentrations of all the other slag constituents were varied only marginally while the temperature was kept constant. As shown in the figure, with an increase in the FeO content, the $\log L_P^{Fe-C}$ value first increased slightly and then decreased. This was in keeping with the phosphorus distribution data for $CaO-FeO-SiO_2-Al_2O_3-Na_2O-TiO_2$ slag and carbon-saturated iron reported by Danaei *et al.*[9] In this study, the maximum $\log L_P^{Fe-C}$ value was observed at FeO contents of 0.6 and 37.5 pct at $R = 2$ [1623 K (1350 °C)] and $R = 1$ [1573 K (1300 °C)], respectively.

However, the difference in the data for these two groups was much larger. The $\log L_P^{Fe-C}$ values for the samples corresponding to experiments 45 to 49 (red solid circles in Figure 8(a)) were much larger than those for the samples corresponding to experiments 16 to 20 (black solid squares in Figure 8(a)), even though the former experiments were performed at a higher temperature [1623 K (1350 °C)]. Further, the minimum value of $\log L_P^{Fe-C}$ for the samples corresponding to experiments 45 to 49 were observed at an FeO content of 15.1 pct; this value was much higher than the maximum value of L_P^{Fe-C} for the samples corresponding to experiments 16 to 20 at an FeO content of 37.5 pct. The reason for this is the fact that the samples in the former group (experiments 45 to 49) exhibited a higher basicity ($R = 2$) than did those in the latter group (experiments 16 to 20, $R = 1$). This further confirmed that, with respect to hot-metal dephosphorization, the basicity of the slag used is a significant factor and has a greater effect than do the oxygen potential and the temperature. The $\log L_P^{Fe-C}$ dependence on the FeO content for the samples with varying compositions (experiments 16 to 54) is shown in Figure 8(b). As can be seen, for FeO contents of 12.3 to 50.6 pct, the L_P^{Fe-C} value did not exhibit a discernable dependence on the FeO content. This suggested that the FeO content in the slag has a weaker effect on L_P^{Fe-C}, and its effect tends to be overshadowed by those of the other factors such as the basicity and temperature. This tendency was observed by Im *et al.* as well,[12] who found that the phosphorus distribution ratio between slag and hot metal showed greater dependence on the CaO content of the slag than on the Fe_tO content at 1573 K (1300 °C).

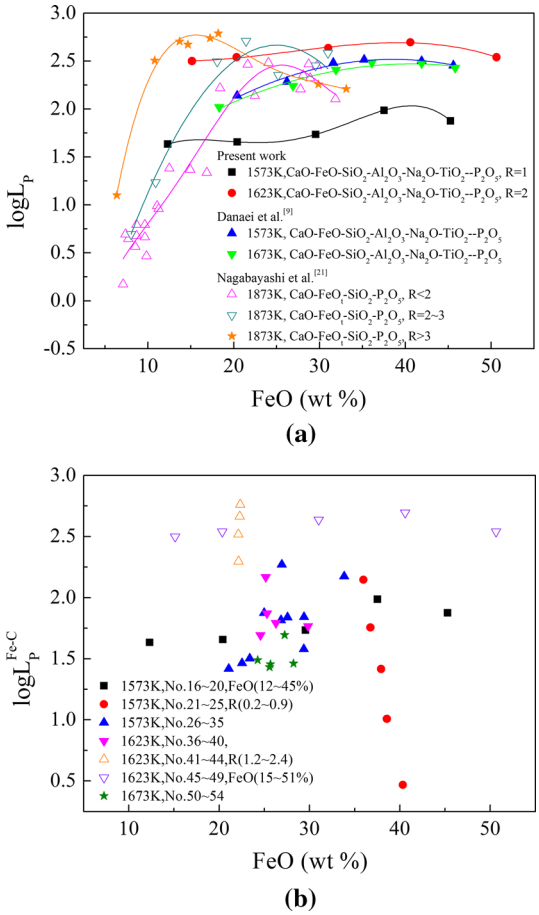

Fig. 8—Effect of FeO on $\log L_P$: (*a*) samples for experiments 16 to 20 and 45 to 49 in Table I and (*b*) samples for experiments 16 to 54 in Table I.

Further, the data in Figure 8(a) from a study by Nagabayashi *et al.*[21] suggests that the phosphorus distribution ratio between slag and molten steel at 1873 K (1600 °C) shows a greater dependence on the FeO content than that observed in this study. Similar results have been reported in other studies[15,22,23] on the dephosphorization of molten steel at approximately 1823 K to 1873 K (1550 °C to 1600 °C). With an increase in the FeO content, the $\log L_P$ value (L_P is the phosphorus distribution ratio between slag and molten steel) first increased sharply and then decreased, with the FeO content corresponding to the maximum value of the phosphorus distribution ratio depending on the slag basicity.

Thus, it can be concluded that the FeO content in slag has a greater effect on the dephosphorization of molten steel than that of hot metal. The reason for this could be as follows. Based on the molecular theory for molten slag, the dephosphorization reaction occurs in two steps: first, the P in the metal phase is oxidized to P_2O_5 by the dissolved oxygen (Eq. [6]). Then the P_2O_5 is fixed in the slag phase by being combined with basic materials such as CaO to form compounds such as $3CaO{\cdot}P_2O_5$ and $4CaO{\cdot}P_2O_5$ (Eq. [7]). Both Eqs. [6] and [7] are

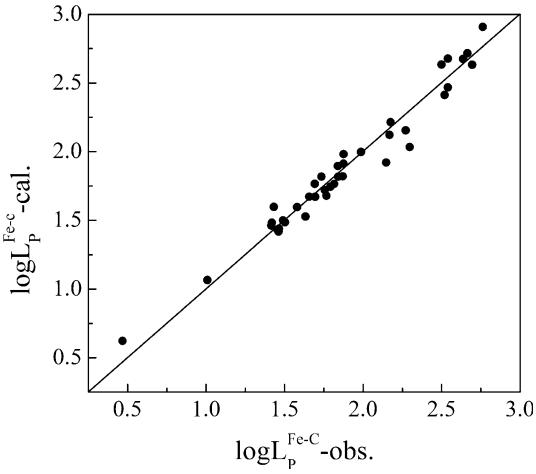

Fig. 9—Comparison of observed values of $\log L_P^{Fe-C}$ and the fitted curve.

exothermic reactions. In the hot-metal stage, because of the high activity coefficient of P (a high carbon content enhances the activity of P in the metal phase) and the relatively low temperature, Eq. [6] moves significantly to the right side even at a lower oxygen potential (which is attributable to the presence of FeO in the slag); in contrast, the fixing of P_2O_5 in the slag phase (Eq. [7]) tends to be the limiting step. Hence, a higher basicity is generally required. However, in molten steel, the oxidization of P through Eq. [6] is not as favorable as in the case of hot metals, owing to the lower activity of P (caused by the extremely low carbon content) and the higher temperature. In this case, a higher oxygen potential is necessary for ensuring that Eq. [6] moves to the right side. Therefore, the FeO content in the slag plays an important role, and phosphorus removal from molten steel is enhanced greatly with an increase in the FeO content. However, the FeO content should not be too high, as this would decrease the amount of free CaO available, thus retarding the reaction in Eq. [7].

$$2[P] + 5[O] = P_2O_5, \qquad [6]$$

$$P_2O_5 + xCaO = xCaO \cdot P_2O_5 \quad (x = 3,\ 4). \qquad [7]$$

F. *Regression Analysis of* L_P^{Fe-C}

Based on the data for experiments 16 to 54 in Table I, the $\log L_P^{Fe-C}$ data were fitted as a function of various factors, including the temperature and those related to the slag composition such as CaO, SiO_2, Al_2O_3, Na_2O, TiO_2, P_2O_5, and FeO contents; this was done using the software SPSS (Statistical Product and Service Solutions).[24] The fitted curve function is given in Eq. [8]. Figure 9 shows both the curve fitted using Eq. [8] and the experimental results; it can be seen that the two agree reasonably well.

$$\log L_P^{Fe-C} = 0.059(\text{pct CaO}) + 1.583\log(\text{TFe}) - 0.052(\text{pct SiO}_2) - 0.014(\text{pct Al}_2\text{O}_3) + 0.142(\text{pct Na}_2\text{O}) - 0.003(\text{pct TiO}_2) + 0.049(\text{pct P}_2\text{O}_5) + \frac{13{,}527}{T} - 9.87, \quad (R = 0.982), \quad [8]$$

where (pct MO) means the concentration (pct mass) of MO in the slag phase.

With respect to the phosphorus distribution ratio between slag and molten steel, L_P, several regression formulas have been proposed previously.[4,25–27]

$$\log\frac{(\text{pct P})}{[\text{pct P}]} = 0.092\{(\text{pct Na}_2\text{O}) + 0.8(\text{pct CaO}) + 0.6(\text{pct MnO}) - 0.9(\text{pct Al}_2\text{O}_3)\} + 2.5\log(\text{TFe}) - 3.54 \quad [9]$$

$$\log\frac{(\text{pct P})}{[\text{pct P}]} = 0.071\{(\text{pct CaO}) + 0.1(\text{pct MgO})\} + \{1.5(\text{pct Na}_2\text{O}) + 4.4\} + 2.5\log(\text{TFe}) + \frac{8260}{T} - 8.65 \quad [10]$$

$$\log\frac{(\text{pct P})}{[\text{pct P}]} = 0.072\{(\text{pct CaO}) + 0.3(\text{pct MgO}) + 0.6(\text{pct P}_2\text{O}_5) + 0.2(\text{pct MnO}) + 1.2(\text{pct CaF}_2) - 0.5(\text{pct Al}_2\text{O}_3)\} + 2.5\log(\text{pct FeO}) + \frac{11,570}{T} - 10.52 \quad [11]$$

$$\log\frac{(\text{pct P})}{[\text{pct P}]} = 0.071\{(\text{pct CaO}) + (\text{pct CaF}_2) + 0.3(\text{pct MgO})\} + 2.5\log[\text{pct O}] + \frac{21{,}740}{T} - 9.87 \quad [12]$$

Equations [9] through [12] were determined through experiments on liquid iron and slags at 1873 K (1600 °C). As can be seen, in all these cases, L_P ($= \frac{(\text{pct P})}{[\text{pct P}]}$, where (pct P) and [pct P] represent the mass fraction of P in the slag and the metal phase, respectively) exhibits a linear dependence on (pct FeO)$^{2.5}$ or (TFe)$^{2.5}$ (here, TFe means the total Fe content in the slag). That is probably owing to the following reasons. The dephosphorization reaction of molten steel can be expressed as shown in Eq. [13], based on the ionic theory of molten slag (*i.e.*, by combining Eqs. [6] and [7]). This suggests that, thermodynamically speaking, a linear relationship between $\frac{(\text{pct P})}{[\text{pct P}]}$ and [pct O]$^{2.5}$ (which represents the oxygen content in the metal phase) holds if one assumes that the activity coefficients of the components of the metal and slag phases remain constant for a given temperature (Eq. [14]). When the slag is in the process of reaching equilibrium with the molten steel, it is assumed that [pct O] is determined by the (pct FeO) value of the slag (Eq. [15]). Accordingly, a linear relationship between L_P and (pct FeO)$^{2.5}$ or (TFe)$^{2.5}$ can be assumed during the removal of phosphorus from molten steel. However, for hot-metal dephosphorization, given the high content carbon of the metal phase, [pct O] is not determined by the (pct FeO) value of the slag any more, since the strong reaction between the carbon and oxygen in the metal phase tends to break the equilibrium state between [O] and (FeO). In this case, $\log L_P^{Fe-C}$ probably shows a linear dependence on [pct O]$^{2.5}$ but not on (pct FeO)$^{2.5}$ any more. During this study, based entirely on the regression analysis of the experimental data and without using any theoretical or thermodynamic models, a linear relationship between L_P^{Fe-C} and (pct FeO)$^{1.583}$ (Eq. [9]) could be obtained. This further confirmed that the FeO content of the slag has a weaker effect on dephosphorization from hot metal with a high carbon content than that on dephosphorization from molten steel.

$$[\text{P}] + \frac{5}{2}[\text{O}] + \frac{3}{2}\left(\text{O}^{2-}\right) = \left(\text{PO}_4^{3-}\right), \quad [13]$$

$$K^{\theta} = \frac{a_{(\text{PO}_4^{3-})}}{a_{[\text{P}]} \cdot a_{[\text{O}]}^{2.5} \cdot a_{(\text{O}^{2-})}^{1.5}}, \quad [14]$$

$$[\text{Fe}] + [\text{O}] = (\text{FeO}), \quad [15]$$

where K^{θ} is the equilibrium constant for Reaction [13], and $a_{(\text{PO}_4^{3-})}$, $a_{[\text{P}]}$, $a_{[\text{O}]}$ and $a_{(\text{O}^{2-})}$ are the activities of PO_4^{3-} in the slag, P in the metal phase, O in the metal phase, and oxygen ions in the slag.

V. CONCLUSIONS

The phosphorus distribution ratios between CaO-FeO-SiO_2-Al_2O_3/Na_2O/TiO_2 slags and carbon-saturated iron were examined in this study. Based on the experimental data gathered, the following conclusions can be drawn.

(1) With the addition of Na_2O and Al_2O_3, the liquid areas in the phase diagram of the CaO-FeO-SiO_2 system are enlarged significantly, with Na_2O having a more pronounced effect than Al_2O_3; on the other hand, TiO_2 has little influence. When used in the proper concentrations, Al_2O_3 and Na_2O can behave as fluxes in the CaO-SiO_2-FeO slag, especially when the binary basicity is high.
(2) The experimental data suggested that L_P^{Fe-C} increases with an increase in the binary basicity of the

slag. Further, L_P^{Fe-C} has a greater dependency on the basicity than on the other influencing factors such as the temperature and FeO content under the conditions investigated in this study.

(3) L_P^{Fe-C} increases with an increase in the Na_2O content and a decrease in the Al_2O_3 content. With an increase in the TiO_2 content, L_P^{Fe-C} decreases slightly; however, the effect of TiO_2 is weaker than that of Al_2O_3.

(4) In contrast to the case for the dephosphorization of molten steel, during hot-metal dephosphorization, the FeO content of the slag has a weaker effect on $\log L_P^{Fe-C}$ than do the other factors such as the temperature and slag basicity under the conditions investigated.

(5) Based on the experimental data, using regression analysis, $\log L_P^{Fe-C}$ could be expressed as a function of the temperature and concentrations of the slag components as follows:

$$\begin{aligned}\log L_P^{Fe-C} = {} & 0.059(\text{pct CaO}) + 1.583\log(\text{TFe}) \\ & - 0.052(\text{pct } SiO_2) - 0.014(\text{pct } Al_2O_3) \\ & + 0.142(\text{pct } Na_2O) - 0.003(\text{pct } TiO_2) \\ & + 0.049(\text{pct } P_2O_5) + \frac{13{,}527}{T} - 9.87, \\ & (R = 0.982).\end{aligned}$$

ACKNOWLEDGMENTS

Financial support for this work was provided by the National Nature Science Foundation of China (Nos. 51474021 and 51674022).

REFERENCES

1. J. Diao: *J. Iron Steel Res.*, 2013, vol. 25, pp. 9–12.
2. G. Li, T. Hamano, and F. Tsukihashi: *ISIJ Int.*, 2005, vol. 45, pp. 12–18.
3. J.J. Pak and R.J. Fruehan: *Metall. Trans. B*, 1991, vol. 22, pp. 39–46.
4. I.H. Jung, J.D. Seo, and S.H. Kim: *Steel Res.*, 2000, vol. 71, pp. 333–39.
5. S.R. Simeonov and N. Sano: *Trans. Iron Steel Inst. Jpn.*, 1985, vol. 25, pp. 1031–35.
6. G. Chen and S. He: *J. S. Afr. Inst. Min. Metall.*, 2014, vol. 114, pp. 391–99.
7. X. Liu, O. Wijk, R. Selin, and J.O. Edström: *ISIJ Int.*, 1998, vol. 38, pp. 36–45.
8. G. Li, C. Zhu, Y. Li, X. Huang, and M. Chen: *Steel Res. Int.*, 2013, vol. 84, pp. 687–94.
9. A. Danaei, Y.D. Yang, M.C. Barati, R. Ravindran, and A. McLean: *Mater. Sci. Technol.*, 2013, vol. 27 (CD only).
10. K. Iwasaki, N. Sano, and Y. Matsushita: *J. Iron Steel Inst. Jpn.*, 1981, vol. 67, pp. 536–40.
11. K. Ito and N. Sano: *J. Iron Steel Inst. Jpn.*, 1983, vol. 69, pp. 1747–54.
12. J. Im, K. Morita, and N. Sano: *ISIJ Int.*, 1996, vol. 36, pp. 517–21.
13. A. Verme and P. Lundh: *Scand. J. Metall.*, 1987, vol. 16, pp. 33–41.
14. P. Spencer and O. Kubaschewski: *Arch. Eisenhüttenwes.*, 1978, vol. 49, pp. 225–28 (in German).
15. H. Ishii and R.J. Fruehan: *Iron Steelmak.*, 1997, vol. 24, pp. 47–54.
16. G. Thornton and D. Anderson: *Ironmak. Steelmak.*, 1994, vol. 21, pp. 247–51.
17. T. Moriya and M. Fujii: *Trans. Iron Steel Inst. Jpn.*, 1981, vol. 21, pp. 732–41.
18. W. Oelsen: *Arch. Eisenhüttenwes.*, 1965, vol. 36, pp. 861–71 (in German).
19. K. Marukawa, Y. Shirota, S. Anezaki, and H. Hirahara: *J. Iron Steel Inst. Jpn.*, 1981, vol. 67, pp. 323–32.
20. J.C. Wrampelmeyer, S. Dimitrov, and D. Janke: *Steel Res.*, 1989, vol. 60, pp. 539–44.
21. R. Nagabayashi, M. Hino, and S. Ban-Ya: *ISIJ Int.*, 1989, vol. 29, pp. 140–47.
22. O. Peter, W. Esche, and W. Oelsen: *Arch. Eisenhüttenwes.*, 1956, vol. 27, pp. 219–30 (in German).
23. H. Knüppel, F. Oeters, and H. Gruß: *Arch. Eisenhüttenwes.*, 1959, vol. 30, pp. 253–65 (in German).
24. R.D. Yockey: *SPSS Demystified: A Step by Step Approach*, Prentice Hall Press, Upper Saddle River, NJ, 2010.
25. K. Kunisada and H. Iwai: *Trans. Iron Steel Inst. Jpn.*, 1987, vol. 27, pp. 263–69.
26. H. Suito and R. Inoue: *ISIJ Int.*, 1995, vol. 35, pp. 258–65.
27. E.T. Turkdogan: *ISIJ Int.*, 2000, vol. 40, pp. 827–32.